Orissa Journal of Physics
ISSN 0974-8202

Vol. 32, No.2
August 2025
pp. 166-178

Structure and Property Correlation in Bismuth Lithium Titanate: A Systematic Analysis

S.S.ROUT[1], A.N.PANI[1], P.S.SAHOO[1†] B.B.MOHANTY[2], S.TRIPATHY[1], M.SAHOO[1] and R.N.P.CHAUDHARY[3]

[1]*Department of Physics, Maharaja Sriram Chandra Bhanj Deo University, Baripada,Odisha, India*

[2]*Department of Physics, Betnoti College Betnoti, Mayurbhanj, Orissa, India*

[3]*Department of Physics, ITER, SOA University, Bhubaneswar, Odisha, India*

[†] Corresponding author. Tel.: +91 889507094

E-mail address: ps rilly@yahoo.com

Abstract: Bismuth lithium titanate (Bi□.□Li□.□TiO□) is synthesized by the conventional solid-state reaction method to examine its structural and electrical behaviour. X-ray diffraction analysis confirms the formation of a single-phase orthorhombic structure, while SEM shows non-uniformly distributed grains over the surface of the pellet sample. Impedance spectroscopy is carried out over broad frequency span (100 Hz–1 MHz) and wide temperature range 30–500 °C. The results indicate that the dielectric and conductivity properties are strongly frequency and temperature-dependent. Activation energy estimated from AC conductivity plots followed Arrhenius behaviour, suggesting mixed-type conduction. The overall study of the compound highlights the correlation between structure and electrical response in bismuth lithium titanate. The impact of frequency and temperature on complex immittance parameters are analyzed by an impedance analyzer in broad frequencies and temperature ranges.

Keywords: X-Ray techniques, Complex-immittance, electrical conductivity, Ceramics, Complex immittance.

1. INTRODUCTION:

The miniaturization of modern electronic devices has a great demand for dielectric materials that offer enhanced performance while enabling compact component design. In multilayer ceramic capacitors, the use of multiple thin dielectric layers is common; however, this complexity can be reduced by employing materials that inherently possess high dielectric constants [1,2]. In this context, barium titanate ($BaTiO_3$, BT), a widely studied perovskite ferroelectric,

has remained a key material due to its large dielectric constant, tunable ferroelectric characteristics, and broad application in capacitors, sensors, memory devices, and other electronic components [3]. In general, high-permittivity dielectric materials are closely linked with ferroelectric or relaxor behaviour, and their dielectric response is strongly influenced by microstructural factors such as grain size [4–6]. Lead zirconate titanate ($Pb(Zr,Ti)O_3$, PZT) has long been considered a benchmark material in piezoelectric applications because of its excellent electromechanical coupling, particularly near the morphotropic phase boundary (MPB) [7]. However, increasing concerns regarding the environmental and health risks associated with lead-based materials have accelerated the search for lead-free alternatives [8,9]. To address this need, several lead-free perovskite-based systems have been widely explored, including potassium sodium niobate ($K_{0.5}Na_{0.5}NbO_3$, KNN), sodium bismuth titanate ($Na_{0.5}Bi_{0.5}TiO_3$, NBT), and $BaTiO_3$-based ceramics [10–12]. Among these, NBT-based materials have gained significant attention due to their relatively high Curie temperature (~380 °C), favorable ferroelectric behaviour, and stable dielectric response. Despite these advantages, issues such as high coercive fields and structural complexity at room temperature still limit their practical use [13–15]. In order to overcome these limitations, various compositional modification strategies have been adopted, including solid-solution formation and aliovalent cation substitution, which can improve densification, lower coercive fields, and enhance piezoelectric/electromechanical performance [16–19]. Lithium substitution has been found to be particularly effective in tailoring ferroelectric behaviour. The incorporation of Li^+ into Bi-based titanates not only provides charge compensation but also introduces structural distortion, which may improve dielectric properties [20]. As a result, $Bi_{0.5}Li_{0.5}TiO_3$ (BLT) has emerged as a promising lead-free ferroelectric material. Earlier studies suggest that BLT can stabilize structural phases, reduce coercive fields, and enhance the dielectric response of composite systems [21–23]. However, detailed understanding of its structural transitions and dielectric behaviour remains limited. Therefore, the present work focuses on the quantitative structural analysis and dielectric characterization of BLT ceramics synthesized via the conventional solid-state reaction route.

2. METHODOLOGY:

2.1: Materials synthesis:

Polycrystalline $Bi_{0.5}Li_{0.5}TiO_3$ (BLT) ceramic is prepared by the conventional solid-state reaction technique. High-purity analytical grade starting materials, namely Bi_2O_3 (99.9%, Central Drug House Pvt. Ltd.), TiO_2 (99.9%, Merck Specialities Pvt. Ltd.), and Li_2CO_3 (99.9%, B.R.M. Enterprises Pvt. Ltd.), are weighed according to the desired stoichiometric composition. The powders are first mixed in air and thoroughly ground using an agate mortar and pestle. To achieve better homogeneity, the mixture is further wet-milled in methanol for 3 h and then dried. The dried powder is then calcined in air at 870 °C for 6 h. Intermediate heating is carried out from 650 °C in steps of 50 °C to facilitate the formation of the required perovskite phase. After calcination, a small amount of binder is added, and then the powder is pressed into pellets under a uniaxial pressure of 4×10^5 N/m². The pellets are then sintered at 880 °C for 6 h to obtain dense ceramics. For electrical measurements, both faces of the sintered pellets are coated with highly conductive silver paste as electrodes. Finally, the samples are annealed at 150 °C for 2 h to remove residual moisture prior to dielectric and electrical characterization.

2.2: MATERIALS CHARACTERIZATION:

The phase formation and quality of the synthesized $Bi_{0.5}Li_{0.5}TiO_3$ (BLT) compound are examined using X-ray diffraction (XRD). The XRD patterns are recorded with an X-ray powder diffractometer (Rigaku Miniflex) using CuKα radiation (λ = 1.540 Å). Data are collected over a range of Bragg angle 2θ = 20°–80° at a scanning rate of 3°/min. The dielectric and impedance behaviour of the fired sample is evaluated using a HIOKI-3532-50 LCR Hi-tester. Measurements are performed in the frequency range of 100 Hz to 1 MHz and within a temperature window of 30 °C to 500 °C.

3. ANALYSIS OF RESULTS:

3.1: Structural & microstructural analysis:

Figure1 gives the development of BLT compound which is characterized using the XRD data.

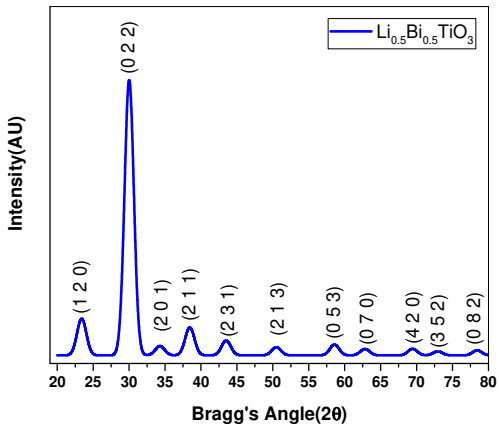

Figure 1. XRD patterns of $Bi_{0.5}Li_{0.5}TiO_3$ (BLT)

Table 1. Calculated and observed value of d-spacing and relative intensities

LBT					
d_{obs}	d_{cal}	H	K	L	I/I_o
3.7983	3.8004	1	2	0	45
2.9760	2.9780	0	2	2	100
2.6129	2.6151	2	0	1	38
2.3398	2.3337	2	2	1	25
2.0786	2.0835	2	3	1	30
1.8064	1.8068	2	1	3	22
1.5747	1.5747	0	5	3	18
1.4780	1.4775	0	7	0	15
1.3522	1.3522	4	2	0	10
1.2957	1.2957	3	5	2	8
1.2183	1.2184	0	8	2	5

Table 2. Cell parameters, volume, and crystallite size of the $Bi_{0.5}Li_{0.5}TiO_3$ compound

Compounds Name	Individual compound	a (Å)	b (Å)	c (Å)	Volume ($Å^3$)	P (nm)
$Bi_{0.5}Li_{0.5}TiO_3$	BLT(x=0)	5.6037(29)	10.3428(29)	7.2852(29)	422.23	8.0266

The XRD pattern of $Bi_{0.5}Li_{0.5}TiO_3$ (BLT) confirms the formation of a single-phase compound without any impurity peaks [24]. All reflection peaks are indexed using POWD-MULT software [25], and the obtained diffraction peaks match well with the reported orthorhombic perovskite structure. Table 1 shows the comparison between the observed (d_{obs}) and calculated (d_{cal}) interplanar spacing values. The close agreement between these values confirms the reliability of the indexing, while the assignment of diffraction peaks to the corresponding (hkl) planes verifies the orthorhombic phase. The (0 2 2) reflection at ~32.5° is identified as the most intense peak, normalized to 100% relative intensity. The absence of additional unindexed peaks further indicates the phase purity of the compound. The refined lattice parameters of the orthorhombic unit cell are obtained as a = 5.6037 Å, b = 10.3428 Å, and c = 7.2852 Å, with a unit cell volume of 422.23 Å³ (Table 2). The average crystallite size, calculated using the Scherrer equation from the (0 2 2) peak, is found to be ~8.02 nm, confirming the nano-crystalline nature of the sample. Although some earlier reports have suggested both tetragonal and orthorhombic phases for BLT [26], the present diffraction pattern clearly supports the orthorhombic structure. This conclusion is good agreement with the observed and calculated d-values, as well as with the peak splitting observed in the diffraction profile [27]. The average crystallite size of the BLT compound is estimated from XRD data using the peak broadening method and Scherrer's relation:

$$D = \frac{k\lambda}{\beta_{1/2}\cos\theta_{Bragg}}$$

where k = 0.89 (shape factor), λ = 1.54 Å (CuKα radiation), and $\beta_1/_2$ is the full width at half maximum of the diffraction peak. The calculated crystallite size is **8.0266×10^{-9} m (≈ 8 nm).**

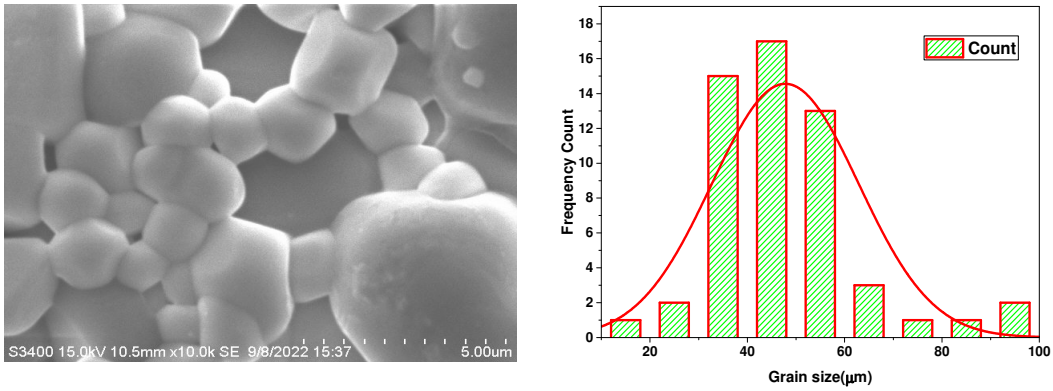

Figure 2. SEM image (left) and Histogram (right) of $Bi_{0.5}Li_{0.5}TiO_3$ (BLT)

Further insight into the microstructure is obtained through SEM analysis. The SEM micrograph (Figure 2, left) shows irregularly shaped grains with clear grain boundaries. The corresponding histogram (Figure 2, right) demonstrates a non-uniform distribution of grain of various sizes across the surface, with the average grain size estimated to be ≈ **68.7 µm.** These results confirm the nanoscale crystallite formation observed by XRD, while SEM reveals the growth and agglomeration of crystallites into larger grains at the microscale.

Figure 3, shows the EDX analysis which confirms the presence of major constituent elements—**bismuth, titanium, and oxygen**—with no detectable impurity peak, indicating the high purity of the synthesized sample. The corresponding elemental composition in terms of weight and atomic percentages is shown in the inset table. Although lithium is a constituent of BLT, it is not observed in the EDX spectrum. This absence is attributed to the **low atomic number of lithium,** which makes it difficult to detect using EDX due to its limited sensitivity to light elements.

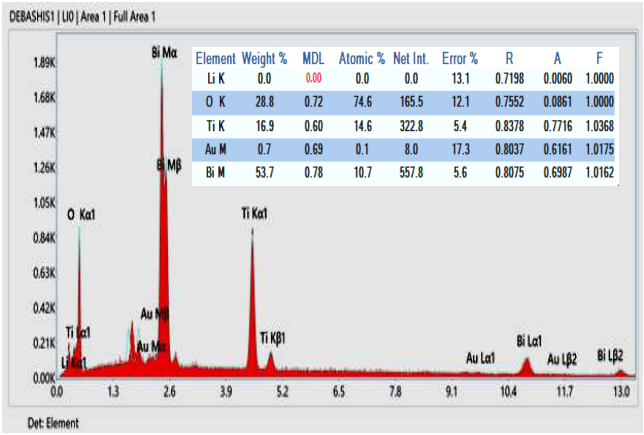

Figure 3. EDX of $Bi_{0.5}Li_{0.5}TiO_3$ (BLT).

3.2 Dielectric Study:

Figure 4 shows the variation of dielectric constant (ε_r) and loss tangent (tan δ) with temperature at different frequencies for the BLT sample. Two dielectric anomalies are observed: the first at ~125 °C, which may correspond to a ferroelectric–antiferroelectric transition, and the second at ~350 °C, which can be attributed to the transition from antiferroelectric to paraelectric phase. Similar anomalies have been reported by other researchers in Bi-based titanates [28, 29].

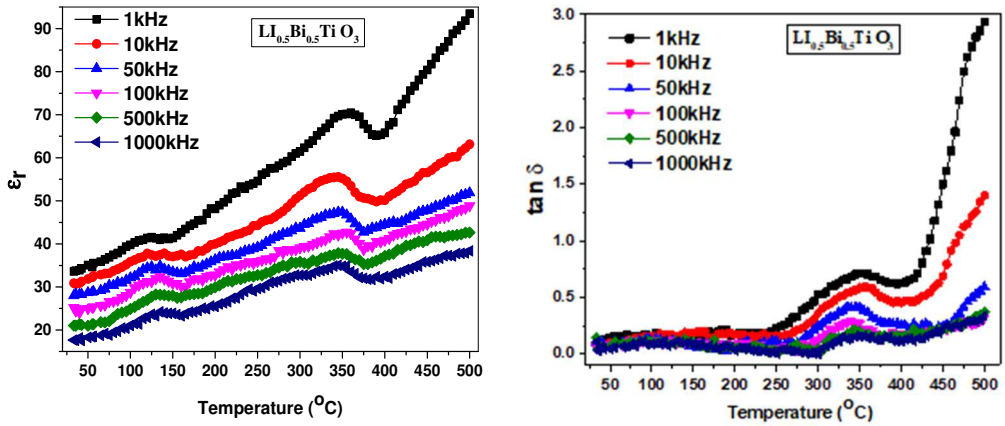

Figure 4. ε_r ~Temperature and Loss tanδ vs temperature for BLT compound.

The dielectric constant (ε_r) decreases with increasing frequency, which is a common characteristic of polar dielectrics. At low frequencies, the high values of ε_r arise due to contributions from space charge, dipolar, ionic, and electronic polarization mechanisms [30,31]. As frequency increases, these polarization contributions cannot keep up with the rapidly oscillating field, leading to a reduction in ε_r. The dielectric loss (tan δ) also exhibits temperature and frequency dependence. At lower temperatures, tan δ is very small, confirming that the material possesses good ferroelectric/insulating properties. With increasing temperature, tan δ increases due to the enhancement of ionic mobility and thermally activated conduction [32]. Peaks in tan δ are observed close to the dielectric anomalies (125 °C and 350 °C), indicating the presence of relaxation processes. These relaxations are particularly pronounced at lower frequencies, which are attributed to grain boundary effects and contributions from dc conductivity [33].

Thus, the dielectric study confirms two distinct phase transitions in BLT and highlights its low dielectric loss in the low-temperature regime, suggesting potential applications in ferroelectric devices.

3.3 Impedance analysis:

Complex immittance spectroscopy (CIS) is considered as the most reliable technique for understanding the electrical behaviour of materials in which multiple processes contribute simultaneously. It is particularly useful for distinguishing the contribution of the bulk (intra-grain) response from that of the bulk–interface or grain-boundary (inter-grain) effects in the overall transport properties of the system.

The complex impedance (Z′–Z″) plots of BLT at selected temperatures are presented in Figure 5 for both low and high temperature regions. In all temperature ranges, the impedance spectra exhibit a single semi-circular arc, indicating that the electrical response is mainly governed by bulk processes within the material. This behaviour can be represented by an equivalent parallel RC circuit. Furthermore, the decrease in resistivity with increasing temperature is evident from the shift of the arc intercepts towards the origin along the real axis. The observed reduction in resistance confirms enhanced bulk conduction at higher temperatures [13].

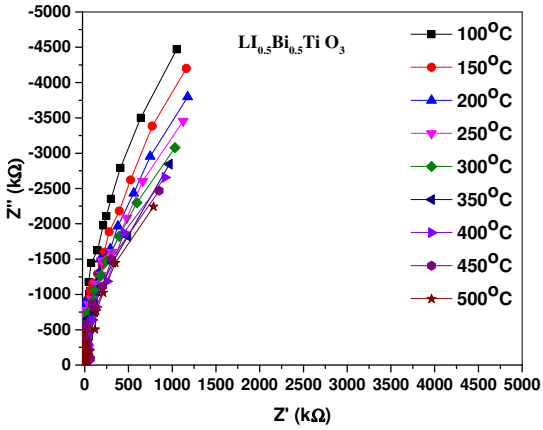

Figure 5. Nyquist plots of $Bi_{0.5}$ $Li_{0.5}TiO_3$ compound at different temperatures

The loss spectra, i.e., the frequency dependence of Z″ for $Bi_{0.5}$ $Li_{0.5}TiO_3$ at different temperatures, are presented in Figure 6(a). At low frequencies, the dispersion observed for all temperatures indicates the involvement of space-charge carriers such as ions, vacancies, and electrons. With increasing frequency, the Z″ values gradually decrease and tend to merge in the high-frequency region, showing a nearly frequency- and temperature-independent behaviour. This merging of the curves at higher frequencies can be attributed to the release of space charges.

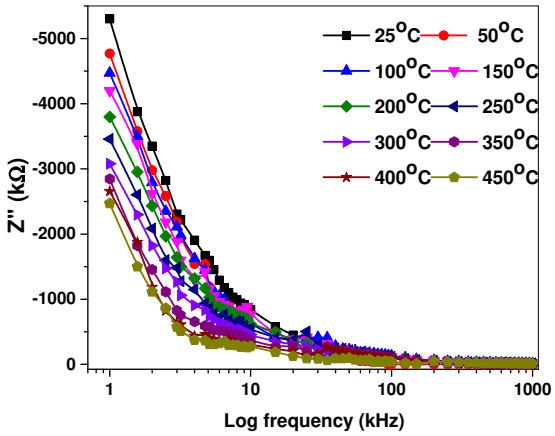

(a)

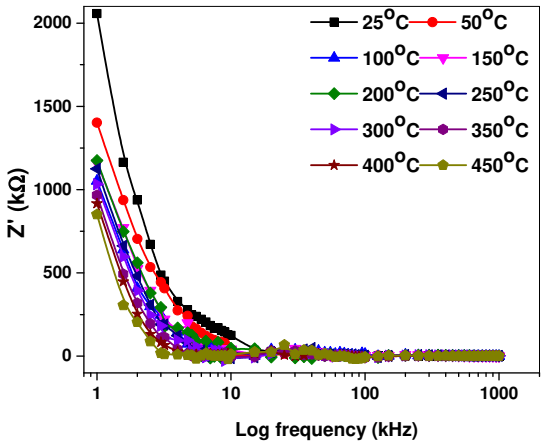

(b)

Figure 6. Frequency-dependent Z′′ (a) and Z′ (b) graphs of $Bi_{0.5}Li_{0.5}TiO_3$ compound at different temperatures

The Z′–frequency plots recorded at different temperatures (25–500 °C) are presented in Figure 6(b). At low frequencies, a spike-like response is observed for almost all temperatures, while with increasing temperature the dispersion becomes more prominent in the high-frequency region. It is also noted that the magnitude of Z′ decreases with rising temperature, indicating NTCR behaviour. Moreover, Z′ shows a significant increase at both low- and high-temperature regions.

3.4 Conductivity study:

The ac conductivity (σ_{ac}) of the BLT sample was calculated using the relation [34] $\sigma_{ac}=\varepsilon_0\varepsilon_r\omega\tan\delta$ where ε_o is the permittivity of free space, εr is the dielectric constant, ω is the angular frequency, and tan δ is the loss tangent.

Figure 7, illustrates the variation of σ_{ac} with inverse absolute temperature (1000/T) at different frequencies. It is observed that σ_{ac} increases with temperature, demonstrating negative temperature coefficient of resistance (NTCR) behavior, which is typical of semiconducting oxides. The conductivity response is divided into three distinct regions. In region-I conductivity is nearly temperature independent, suggesting localized hopping of charge carriers, in region-II conductivity increases rapidly with temperature, indicating a thermally activated process, and in region-III conductivity again shows weaker temperature dependence, implying saturation of carrier mobility.

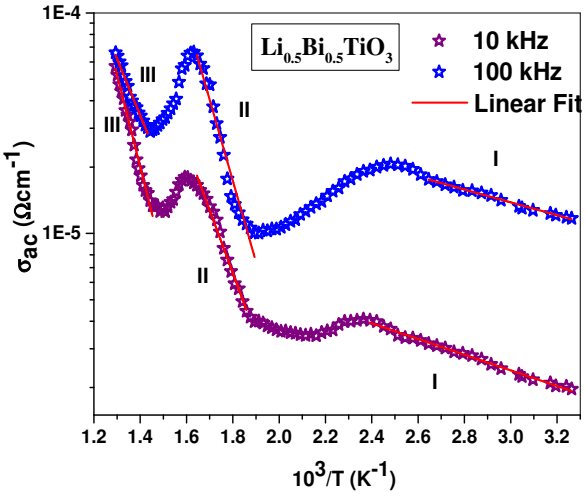

Figure 7. Variation of ac conductivity with the temperature of BLT compound.

Table 3. Value of activation energies in different frequency regions

Compounds name	Individual Compound	Frequencies	Activation energy E_a (eV)		
			Region-I	Region-II	Region-III
$Li_{0.5}Bi_{0.5}TiO_3$	LBT(x=0)	10 kHz	0.07054	0.56629	0.82848
		100 kHz	0,04008	0.72965	0.50915

The activation energy (EaE_aEa) is evaluated using the Arrhenius relation $\sigma_{ac}=\sigma_0 \exp\ (-Ea/kBT)$. The calculated E_a values (Table 3) vary with frequency and temperature, indicating different conduction mechanisms in different regions. Lower E_a at low temperatures suggests excitation of localized charge carriers, whereas higher E_a at elevated temperatures is attributed to long-range ionic migration and grain-boundary conduction. The merging of σ_{ac} plots at high temperatures into a master curve indicates frequency-independent conduction in this region.

4. CONCLUSIONS:

Polycrystalline $Bi_{0.5}Li_{0.5}TiO_3$ (BLT) ceramics is successfully synthesized by the solid-state reaction route. XRD confirms a single-phase orthorhombic perovskite structure with nanoscale crystallite size, while SEM/EDX shows irregular grains size, non-uniform distribution, and no impurity phases. Dielectric studies revealed anomalies near 125 °C and 350°C, associated with ferroelectric–antiferroelectric and antiferroelectric–paraelectric transitions. The dielectric constant shows strong frequency dispersion with low loss at low temperatures. AC conductivity follows Arrhenius behaviour and Jonscher's power law, indicating multiple conduction mechanisms with NTCR behaviour. The Z′–Z″ plots exhibit single semicircular arcs, suggesting dominant bulk contribution. In overall, BLT exhibits potential application for lead-free electronic devices such as thermistors, capacitors, sensors, and energy-storage devices.

REFERENCE:

[1] Uchino K. *Ferroelectric Devices*. CRC Press, 2000.

[2] Jaffe B., Cook W.R., Jaffe H. *Piezoelectric Ceramics*. Academic Press, 1971.

[3] Lines M.E., Glass A.M. *Principles and Applications of Ferroelectrics and Related Materials*. Clarendon Press, 1977.

[4] Shrout T.R., Zhang S.J. Lead-free piezoelectric ceramics: Alternatives for PZT? *J. Electroceram.* 2007, 19:113–126.

[5] Xu Y. *Ferroelectric Materials and Their Applications*. Elsevier, 1991.

[6] Damjanovic D. Ferroelectric, dielectric and piezoelectric properties of ferroelectric thin films and ceramics. *Rep. Prog. Phys.* 1998, 61:1267–1324.

[7] Noheda B. Structure and high-piezoelectricity in lead oxide solid solutions. *Curr. Opin. Solid State Mater. Sci.* 2002, 6:27–34.

[8] Rödel J., et al. Perspective on the development of lead-free piezoceramics. *J. Am. Ceram. Soc.* 2009, 92:1153–1177.

[9] Panda P.K. Review: Environmental friendly lead-free piezoelectric materials. *J. Mater. Sci.* 2009, 44:5049–5062.

[10] Saito Y., et al. Lead-free piezoceramics. *Nature* 2004, 432:84–87.

[11] Takenaka T., Nagata H. Current status and prospects of lead-free piezoelectric ceramics. *J. Eur. Ceram. Soc.* 2005, 25:2693–2700.

[12] Shrout T.R., Zhang S.J. Relaxor-PbTiO□ single crystals and related materials. *J. Electroceram.* 2007, 19:111–124.

[13] Takenaka T., Maruyama K., Sakata K. (Bi□.□Na□.□)TiO□–BaTiO□ system for lead-free piezoelectric ceramics. *Jpn. J. Appl. Phys.* 1991, 30:2236–2239.

[14] Zhang S.J., Li F. High performance ferroelectric relaxor-PbTiO□ single crystals: Status and perspective. *J. Appl. Phys.* 2012, 111:031301.

[15] Jo W., Rödel J. Electric-field-induced volume change and phase transitions of (Bi□/□Na□/□)TiO□-based lead-free piezoceramics. *Appl. Phys. Lett.* 2012, 100:252904.

[16] Zhou C., et al. Effects of lithium substitution on structural and electrical properties of NBT ceramics. *Ceram. Int.* 2014, 40:13051–13056.

[17] Xiang H., et al. Lithium substitution effects in (Bi□.□Na□.□)TiO□–BaTiO□ ceramics. *J. Eur. Ceram. Soc.* 2012, 32:1161–1167.

[18] Wu J., Xiao D., Zhu J. Potassium–sodium niobate lead-free piezoelectric materials: Past, present, and future. *J. Adv. Dielectr.* 2013, 3:1330001.

[19] Rödel J., Jo W., Seifert K.T., Anton E.M., Granzow T., Damjanovic D. Perspective on the development of lead-free piezoceramics: Pb-free systems. *J. Am. Ceram. Soc.* 2009, 92:1153–1177.

[20] Panigrahi M.R., Rout D., Pradhan D.K. Structural and dielectric properties of lithium-modified bismuth titanate ceramics. *Mater. Res. Bull.* 2014, 50:416–421.

[21] Wu J., Xiao D., Zhu J. Progress in lead-free piezoelectric materials: Sodium potassium niobate. *J. Mater. Sci.* 2015, 50:4331–4352.

[22] Pradhan D.K., Panigrahi M.R., et al. Effect of Li incorporation on Bi-based ferroelectrics. *J. Alloys Compd.* 2013, 580:123–129.

[23] Nayak M., Panigrahi M.R. Quantitative structural analysis of Bi□.□Li□.□TiO□ ceramics. *J. Mater. Sci.: Mater. Electron.* 2016, 27:8312–8318.

[24] P. S. Sahoo, B. B. Mohanty, J. Panda, and R. N. P. Choudhary 2014 *Res. Inventry* vol **4** (12) p 38.
[25] B.B. Mohanty, P. S. Sahoo, Mahapatra P.K Sahoo, and R. N. P. Choudhary, Synthesis and electrical analysis of $Ba_5GdTi_3V_7O_{30}$ ceramics , J. Materials science and application 3,(2013),173-178.
[26] G. Nalini, and T. N. Guru Row 2002 *J.Bull.Mater Sci.* vol 25 pp 275-281.
[27] H. Irie, M. Miyayama, and T. Kudo 2001 *J.Appl.Phys* vol 90,8 pp 4089-4094.
[28] P. Julphunthong, T. Bongkarn, and S. Maensiri, Ceram. Int. 41, 143 (2015).
[29] M. Nayak1, and Manas R. Panigrahi J Mater Sci: Mater Electron (2016) 27:8312–8318.
[30] C. Kittel, *"Introduction to Solid State Physics"*, Wiley, 5th Edition, New York (1976).
[31] Swagatika Dash, R. Padhee, Piyush R. Das, and R.N.P. Choudhary, Phase Transitions **87.**
[32] P. S. Sahoo , A. Panigrahi , S. K. Patri, and R. N. P. Choudhary 2009 *Materials Letter* vol 63 (11) pp 864-866.
[33] O. Raymond, R. Font, N. Suárez-Almodovar, J.Portelles, and J. M. Siqueiros, *J. Appl.Phy.*, 97; 084107(2005).
[34] R Moos and K H Härdtl 1996 *Journal of applied Physics* vol 80(1) p 393.
[35] A. K. Jonscher 1977 *Nature* vol 267 p 673.